

Towards a Controlled Orthosis for Sit-To-Stand Support in Independently Living Elderly: Model Development

Jasper Juchem* Mia Loccufier* Amélie Chevalier*,**,***

* Department of Electromechanical, Systems and Metals Engineering, Ghent University, 9052 Gent, Belgium (e-mail: {Jasper.Juchem, Mia.Loccufier, Amelie.Chevalier}@UGent.be)

** Department of Electromechanics, CoSysLab, University of Antwerp, Belgium

*** AnSyMo/Cosys, Flanders Make, the strategic research centre for the manufacturing industry

Abstract: Sit-to-stand (STS) movements are a daily challenge for independently living elderly. Literature shows a keen interest in using active orthoses to mitigate this problem. However, to design and test advanced control strategies for proof-of-concept orthoses, a validated model of the STS movement is missing. This work presents and elaborates on a model of the kinematics of the lower limb in combination with a human policy which represents the brain-muscle interaction. The model parameters are derived from both healthy and elderly patients. The applicability of the model is investigated by applying two popular control methods for active orthoses: gravity compensation and a control-based method. First, the results show model validation using measured *in vivo* joint torques from literature and, second, that both methods can be simulated using the developed STS model. This allows for optimizing and testing advanced control strategies in future work.

Copyright © 2023 The Authors. This is an open access article under the CC BY-NC-ND license (<https://creativecommons.org/licenses/by-nc-nd/4.0/>)

Keywords: orthosis, sit-to-stand, model development, elderly

1. INTRODUCTION

The elderly often suffer from gait and balance disorders resulting in injuring falls (Pirker and Katzenschlager (2017)). The fear of falling has a crippling effect with loss of independence and consequently reduction of quality of life (Schoene et al. (2019)). Moreover, cutting down physical training deteriorates muscle and balance function even further. This is why elderly must keep exercising to regain this muscle and balance function (Oddsson et al. (2007)).

An example of a daily task that becomes more difficult with age, is the sit-to-stand (STS) movement (dos Santos et al. (2011); Sadeghi et al. (2013)). For people of age, this movement is not that straightforward and they often need additional support, like a walker, to rise up from a chair.

An orthosis could help the elderly to perform this motion in a more natural way, both to regain confidence in the movement and to train their muscles (Esquenazi and Talaty (2019)). Ideally, the elderly could perform this training without a physical therapist having to be present at all times (Gorgey et al. (2019)). Therefore, the orthosis should be easy to wear and accessible at home.

Despite the extensive literature in the design and validation of lower limb exoskeletons of which some can also be incorporated in rehabilitation (Shepherd and Rouse (2017); Sheng et al. (2022)), no devices are commercially available. In Shepherd and Rouse (2017), the sit-to-stand motion is addressed for post-stroke patients with asym-

metrical leg muscle power. The mechanical design of the orthosis is the focus in Shepherd and Rouse (2017).

In all the designs in literature, determining a torque reference trajectory to the controller is challenging as real-time Electromyography (EMG) on diseased patients might not yield realistic trajectories. Therefore, EMG data on healthy patients reported in literature (Roebroek et al. (1994)) are used as basis to determine the torque references. Testing the prototypes of the new orthosis designs is done on healthy volunteers (Shepherd and Rouse (2017)). This shows the need for a simulation tool to predict the kinematic behavior of an elderly person using the new orthosis prototypes. The orthosis from Shepherd and Rouse (2017) has the limitation of only acting on the knee joint and not the ankle joint as well. Therefore, a model which allows to simulate actuation on more than one joint for the STS movement might yield improvements in the field of orthoses.

The lack of a good simulator for the STS movement in the elderly is mediated in this work. The simulator will allow future researchers to test new advanced control strategies for active orthoses and to simulate and investigate torque trajectories for the elderly. A model is developed which represents the STS movement performed by a healthy person, i.e. someone who is able to perform a STS without limitations, and a person of age, i.e. a person who is not able to perform a STS movement without any form of assistance. This model has two important aspects, namely

how the body moves as a reaction of the contracting muscles, i.e. lower limb kinematics, and how the muscles are activated by the brain and nervous system, i.e. the human policy. This combination is unique and enhances the state-of-the-art on STS models. The model includes the ankle, knee and hip joint, allowing future orthosis designs to choose one, two or three actuators.

The structure of this paper is as follows: Section 2 presents the models of the healthy person and the adaptation for elderly. The use of the simulator is shown by implementing two popular control strategies. The simulation results are presented in Section 3 along with the discussion and the limitations. A conclusion is formed in a final section.

2. MATERIALS AND METHODS

The block diagram of the complete model is shown in Fig. 1. Each block will be explained separately in the following subsections.

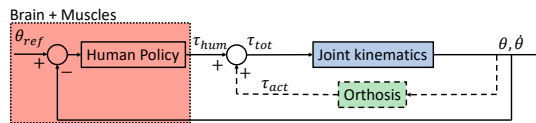


Fig. 1. Block diagram of the STS simulator.

2.1 Kinematic model

A model for the sit-to-stand movement is developed. To be able to accurately observe the joint torques required for this action, it is assumed there is no extra support available and the hands are not used to push the body upwards. In the initial position, the upper body is up straight and thus makes a 90° angle with the horizontal, the knees are bent, the shins are tilted a bit forward and the feet are put flat on the ground as depicted in Fig. 2. Looking at the definition of the joint angles θ_i in Fig. 2, the initial position used for this research is $\theta_1 = 80^\circ$, $\theta_2 = 161^\circ$ and $\theta_3 = 90^\circ$. The ultimate goal of the sit-to-stand movement is to end up in the upright position, which is equivalent to the upper body, thighs and shins making an angle of 90° with the horizontal reference. The feet are flat on the ground.

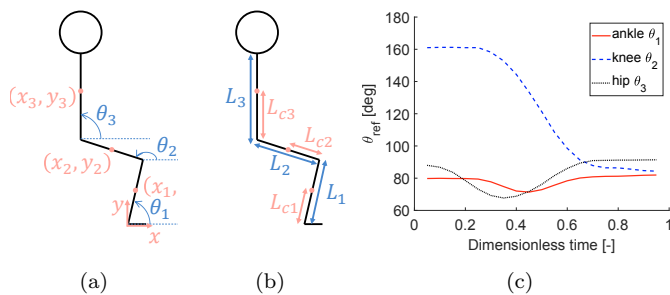


Fig. 2. Definition of (a) the frame of reference with the joint angles and (b) the lengths and distances. (c) show the reference trajectories for θ_1 , θ_2 and θ_3 , based on Sadeghi et al. (2013).

Sadeghi et al. (2013) defined reference joint angles of a healthy person performing the sit-to-stand movement shown in Fig. 2c.

The lower limb kinematics are modeled as a three-link pendulum (Sadeghi et al. (2013)) carrying half of the upper body weight, as the movement is assumed to be symmetric for the left and right leg.

The three-link model transforms the joint torques, caused by contraction of the muscles, to a movement of the human body. The three-link pendulum with its reference angles and parameters is given in Fig. 2. The equations of motion of the shank, thigh and upper body are obtained using the Euler-Lagrange formalism

$$M(\theta) \cdot \ddot{\theta} + C(\theta, \dot{\theta}) \cdot \dot{\theta} + G(\theta) = B \cdot \tau + J \cdot F_{ext}. \quad (1)$$

with $\theta = [\theta_1 \ \theta_2 \ \theta_3]^T$ and $\tau \in \mathbb{R}^3$. The angles θ_i are defined as in Fig. 2 and the joint torques τ are defined in the same sense as those angles. These joint torques are related to the movement of the shank, thigh and upper body by the matrix $B \in \mathbb{R}^{3 \times 3}$. The matrix $M \in \mathbb{R}^{3 \times 3}$ is the inertia matrix, $C \in \mathbb{R}^{3 \times 3}$ the matrix containing Coriolis and centripetal terms and $G \in \mathbb{R}^3$ the gravitational vector. External forces can be comprised in $F_{ext} \in \mathbb{R}^3$ and are mapped onto torques and related to the movements by the matrix $J \in \mathbb{R}^3$.

The bio-mechanical parameters, such as mass m_i , length L_i , position of the center of mass L_{ci} , and the moment of inertia I_i of the body segments, are estimated using the segment inertia parameters defined by de Leva (1996). Combining these parameters with the parallel axis theorem and the method to find the center of mass of combined bodies, the segment parameters of the shank, thigh and upper body are obtained (see Table 1).

Table 1. Adapted segment parameters for the shank, thigh and upper body.

	m_i (kg)	L_i (m)	L_{ci} (m)	I_i (kg · m ²)
Shank (i=1)	3.23	0.434	0.241	0.038
Thigh (i=2)	10.62	0.422	0.249	0.205
Upper body (i=3)	45.21	0.735	0.368	2.642

The force exerted by the chair is modeled in the term F_{ext} . Literature proposes a way to include the chair force in the model by simplifying the chair to a mass and damper system exerting force in the vertical direction (Sadeghi et al. (2013)). With this information, the matrix J can be constructed. Taking this insight and building upon the structure of the chair equations in Sadeghi et al. (2013), the chair force will be mathematically represented by an exponential model in this research:

$$F_{ext} = A \cdot \exp(-a(y_{hip} - y_0)) \quad (2)$$

with y_{hip} the height of the hip joint. This particular height can be calculated in function of the angles θ_i and the bio-mechanical parameters using trigonometry. Other unknowns in (2) are all fixed parameters, such as the amplitude A , the scaling constant a and the height of the chair when it is relaxed y_0 .

2.2 Human policy

The human policy represents how the human brain creates a control signal that constitutes the torque profiles and how it is transmitted by the nervous system and later executed by the muscles, resulting in the required torques. It requires information about the current state of the

system, being the angles θ_i and angular velocities $\dot{\theta}_i$ and a θ_{ref} , which is a reference trajectory for the angles θ_i generated by the brain. This reference trajectory is not an actual input in practice, but rather a learned movement. To transform those inputs into the required joint torques τ_i , Lv and Gregg (2018) propose the following dynamic equation:

$$\tau = K_p \cdot e - K_d \cdot \dot{\theta}. \quad (3)$$

In this equation the error signal $e \in \mathbb{R}^3$ is equal to $e = \theta_{ref} - \theta$. The matrices K_p and $K_d \in \mathbb{R}^{3 \times 3}$ are the stiffness and damping matrices, respectively. The choice of this dynamic equation (3) is based on insights on how neural networks learn the nominal walking trajectories in biped robots (Lv and Gregg (2018); Braun and Goldfarb (2009)). However, this work validates whether this insight is also applicable in human subjects.

Validation of the PD assumption is done by linearizing the three-link model around the unstable equilibrium point $[\theta_1, \theta_2, \theta_3, \dot{\theta}_1, \dot{\theta}_2, \dot{\theta}_3] = [\frac{\pi}{2}, \frac{\pi}{2}, \frac{\pi}{2}, 0, 0, 0]$. This linearization results in three transfer functions from τ_i to θ_i with 4 zeros and 6 poles.

The work of Sadeghi et al. (2013) provides an experimental dataset for the joint angles and the joint torques. The entire loop, as given in Fig. 1 without the orthosis present, can be summarized to a single block with input θ_{ref} and output τ_{hum} :

$$\frac{\tau_{hum}}{\theta_{ref}} = \frac{HP(s)}{1 + HP(s) \frac{(s+z_1)\dots(s+z_4)}{(s+p_1)\dots(s+p_6)}} \quad (4)$$

with $HP(s)$ the dynamics of the human policy. Using the system identification method *ARX* (Ljung (1983)), the transfer function $\frac{\tau_{hum}}{\theta_{ref}}$ can be identified based on the input-output relationship from Sadeghi et al. (2013). From the identified number of poles and zeros in the complete transfer function, the number of poles and zeros in the human policy $HP(s)$ can be calculated using (4).

The complete transfer function identification yields 7 zeros and 6 poles. Fig. 3 compares the experimental data from Sadeghi et al. (2013) with the estimated model with 7 zeros and 6 poles. It also gives the percentage of fit. The result of 7 zeros and 6 poles is the point at which adding extra poles or zeros to the optimization process did not yield in an additional improvement in percentage of fit. From this optimization of the number of poles and zeros in the complete transfer function, the structure of the human policy $HP(s)$ is calculated as:

$$\frac{\tau_{hum}}{\theta_{ref}} = Q \frac{(s+z_1)\dots(s+z_7)}{(s+p_1)\dots(s+p_6)} = \frac{HP(s)}{1 + HP(s) \frac{(s+z_1)\dots(s+z_4)}{(s+p_1)\dots(s+p_6)}} \quad (5)$$

which yields:

$$HP(s) = K(s+z) \quad (6)$$

This shows that the assumption of a PD structure for the human policy is reasonable.

The next step is tuning the human policy parameters, i.e. the matrices K_p and K_d in (3). A deviation in one of the joint angles θ_i from its reference angle $\theta_{ref,i}$ will only influence the actual trajectory of that joint angle. With this simplification, the final equation to represent the human policy becomes:

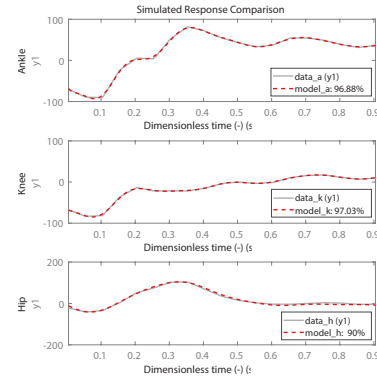


Fig. 3. Comparison of the estimated model and the experimental data from Sadeghi et al. (2013) for the transfer function with $\theta_{ref,i}$ as input and output τ_i for the (a) ankle, (b) knee and (c) hip.

$$B \cdot \begin{bmatrix} \tau_1 \\ \tau_2 \\ \tau_3 \end{bmatrix} = \begin{bmatrix} K_{p,1} & 0 & 0 \\ 0 & K_{p,2} & 0 \\ 0 & 0 & K_{p,3} \end{bmatrix} \begin{bmatrix} \theta_{ref,1} - \theta_1 \\ \theta_{ref,2} - \theta_2 \\ \theta_{ref,3} - \theta_3 \end{bmatrix} - \begin{bmatrix} K_{d,1} & 0 & 0 \\ 0 & K_{d,2} & 0 \\ 0 & 0 & K_{d,3} \end{bmatrix} \begin{bmatrix} \dot{\theta}_1 \\ \dot{\theta}_2 \\ \dot{\theta}_3 \end{bmatrix} + B \cdot \begin{bmatrix} Z_1 \\ Z_2 \\ Z_3 \end{bmatrix} \quad (7)$$

An extra gravitation compensation term needs to be added such that in equilibrium ($\theta = 0, \dot{\theta} = 0$) (1) results in $\theta_{eq} = \theta_{ref}$:

$$\begin{cases} g(m_1 L_{c1} + m_2 L_1) \cos(\theta_{eq,1}) + L_1 \cos(\theta_{eq,1}) F_{ext}(\theta_{eq}) \\ = K_{p,1}(\theta_{ref,1} - \theta_{eq,1}) + Z_1 - Z_2 \\ g(m_2 L_{c2} + m_3 L_2) \cos(\theta_{eq,2}) + L_2 \cos(\theta_{eq,2}) F_{ext}(\theta_{eq}) \\ = K_{p,2}(\theta_{ref,2} - \theta_{eq,2}) + Z_2 - Z_3 \\ gm_3 L_{c3} \cos(\theta_{eq,3}) = K_{p,3}(\theta_{ref,3} - \theta_{eq,3}) + Z_3 \end{cases} \quad (8)$$

To do this, the compensation term is chosen to be

$$Z = [Z_1 \ Z_2 \ Z_3]^T = B^{-1} \cdot K(\theta_{ref}) \quad (9)$$

with

$$K(\theta) = G(\theta) - J(\theta) \cdot F_{ext}. \quad (10)$$

To tune the parameters of K_p and K_d the following aspects are considered. First, to avoid oscillatory trajectories towards equilibrium, which is unlikely as the brain is able to steer the muscles such that the STS movement stays close to the intended trajectory for a healthy person, K_d should be taken high enough. Second, the closed-loop system can possess multiple equilibrium points. However, there should be a unique equilibrium point. For proper operation the last equation of (8) can be written as

$$gm_3 L_{c3} \cos(\theta_{eq,3}) = c_3 - K_{p,3} \theta_{eq,3} \quad (11)$$

where all constant terms are comprised in c_3 . If $K_{p,3}$ is too small, multiple equilibrium points exist, so it is paramount to take it sufficiently high. The same holds for all equations in (8). A lower limit can be defined by the absolute value of the derivative of the left-hand term

$$\begin{cases} K_{p,1} \gg g(m_1 L_{c1} + m_2 L_1 + m_3 L_1) \\ K_{p,2} \gg g(m_2 L_{c2} + m_3 L_2) \\ K_{p,3} \gg gm_3 L_{c3} \end{cases} \quad (12)$$

Third, K_p and K_d have an upper limit. If they are chosen too high the P-action and the D-action in (7) will become large as well. As these two large terms will be subtracted this will lead to a nervous behaviour, which is unwanted.

Table 2. Tuned parameters for K_p and K_d representing the human policy.

	$K_{p,i}$	$K_{d,i}$
$i = 1$	3000	100
$i = 2$	3840	100
$i = 3$	3608	100

To obtain numeric values for K_p and K_d the relative error $e_{rel} = (\theta_{ref} - \theta) / \theta_{ref}$ is minimized manually to obtain acceptable torques, based on the *in vivo* data. This results in the values in Table 2.

2.3 The elderly

The elderly often have a reduced muscle function and a decrease of cartilage, and thus damping. These two aspects of physical weakness that accompany old age can be represented within the human policy. The stiffness matrix K_p and the damping matrix K_d represent the amount of muscle function and damping capacity, respectively. Decreasing these values can give an accurate representation of what happens with old age. Important to note is that not all joints and muscles deteriorate at the same speed with old age. In most cases the knee torque experiences a greater reduction than the ankle and hip torque (DeVita and Hortobagyi (2000)). For this reason, the remaining capacity of the ankle and hip joint is chosen at 88%, and for the knee this is set at 78% (Gross et al. (1998)). This results in the following:

$$B \cdot K_p = \begin{bmatrix} 0.88K_{p,1} & 0 & 0 \\ 0 & 0.78K_{p,2} & 0 \\ 0 & 0 & 0.88K_{p,3} \end{bmatrix} \quad (13)$$

The reduction in the damping matrix K_d was kept at 20 % for all joints. Furthermore, the maximal attainable torque is limited using a saturation function, which is patient specific. Here, the maximal torque is reduced with 20% to show the effect of the lower capabilities.

2.4 Model application: closed loop control

This model is developed for the design of advanced control strategies for orthosis helping the elderly with STS movements. Therefore, it is useful to illustrate its application using two popular methods: a gravity compensation method (Lv and Gregg (2018)) and a control-based approach (Rajasekaran et al. (2017)). Both the block diagrams are shown in Fig. 4.

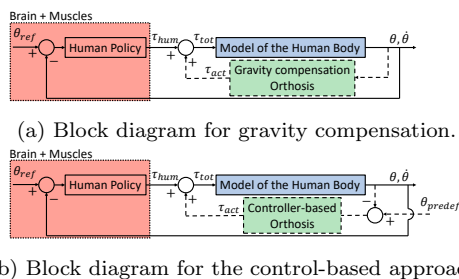


Fig. 4. Block diagrams of the closed loop control.

Gravity compensation The gravity compensation method aims to make the wearer experience a reduced gravity force, contained within the term G in (1) (Fig. 4a). It

has only been developed for gait movements in previous research (Lv and Gregg (2018)). In this paragraph the gravity compensation method is developed for STS movements.

Experiencing a smaller gravity force is equivalent to experiencing a smaller gravity constant $\tilde{g} = \mu g$, where μ is a reduction factor, which can be adapted based on the amount of force the user can provide. Using this alternative gravity constant results in an alternative gravity vector $\tilde{G} = \mu G$. To find the required actuator torques that need to be delivered by the orthosis in the ankle and knee, a matching condition should be found. First, it is known that the equations of motion while wearing an orthosis are given by

$$M(\theta) \cdot \ddot{\theta} + C(\theta, \dot{\theta}) \cdot \dot{\theta} + G(\theta) = B \cdot \tau + B' \cdot \tau_{act} + J(\theta) \cdot F_{ch}(\theta) \quad (14)$$

with the actuator torques $\tau_{act} \in \mathbb{R}^2$ solely present at the ankle and knee, and $B' \in \mathbb{R}^{3 \times 2}$ maps these torques onto the motions of body segments. Second, the equations of motion as experienced by the wearer are

$$M(\theta) \cdot \ddot{\theta} + C(\theta, \dot{\theta}) \cdot \dot{\theta} + \tilde{G}(\theta) = B \cdot \tau + J(\theta) \cdot F_{ch}(\theta). \quad (15)$$

For (14) and (15) to be equivalent, the following matching condition should be satisfied:

$$B' \tau_{act} = G(\theta) - \tilde{G}(\theta). \quad (16)$$

Since B' is not square, the matrix is not invertible. Therefore, an approximate inverse, namely the Moore-Penrose or pseudo-inverse (Courrieu (2008)) $B^+ = (B^T \cdot B)^{-1} B^T$ is used.

With this, the actuator torques can be found as:

$$\begin{bmatrix} \tau_{act,1} \\ \tau_{act,2} \end{bmatrix} = (1 - \mu)g \begin{bmatrix} 1 & 1 & 0 \\ 0 & 1 & 0 \end{bmatrix} \cdot \begin{bmatrix} (m_1 L_{c1} + m_2 L_1 + m_3 L_1) \cos(\theta_1) \\ (m_2 L_{c2} + m_3 L_2) \cos(\theta_2) \\ m_3 L_{c3} \cos(\theta_3) \end{bmatrix}. \quad (17)$$

A value for μ should be tuned to help the wearer in the best way possible. This is a patient specific parameter, since each person can have a different reduction in muscle and damping function. For the situation studied in this research $\mu = 0.8$ is found to be suitable. Note here that the gravitation method highly depends on the model accuracy. An alternative is a control-based approach.

Control-based approach The example of control-based approach chosen in this illustration is a PD-controller (Fig. 4b). A PD-controller requires a predefined reference signal. This predefined reference signal is denoted as θ_{predef} and is taken equal to θ_{ref} for the simulations. In practice, this trajectory will be patient specific and will probably not be equal to the signal generated by the brain. As there are no actuators and sensors on the hip, the signal θ_3 will be replaced with a constant value, namely the initial and final value $\frac{\pi}{2}$ rad. Because θ_3 will be replaced by a constant, $\dot{\theta}_3$ becomes zero at all times. The final equation for the controller that will be used in the orthosis is given in (18).

$$\begin{bmatrix} \tau_{act,1} \\ \tau_{act,2} \end{bmatrix} = \begin{bmatrix} P_1 & P_2 & P_3 \\ 0 & P_2 & P_3 \end{bmatrix} \begin{bmatrix} \theta_{predef,1} - \theta_1 \\ \theta_{predef,2} - \theta_2 \\ \theta_{predef,3} - \frac{\pi}{2} \end{bmatrix} - \begin{bmatrix} D_1 & D_2 & D_3 \\ 0 & D_2 & D_3 \end{bmatrix} \begin{bmatrix} \dot{\theta}_1 \\ \dot{\theta}_2 \\ 0 \end{bmatrix} \quad (18)$$

The values of P_i and D_i are tuned to limit the relative joint angle errors e_{rel} to a minimum, while respecting the physical restraints of the human body. The numerical

values are $\{P_1, P_2, P_3\} = \{70, 140, 12\}$ and $D_i = 0.5$ for all $i \in \{1, 2, 3\}$.

3. RESULTS AND DISCUSSION

3.1 Kinematic model validation

The model of the lower limb kinematics including the chair and the defined biomechanical parameters is validated using joint torques reported in literature from Gross et al. (1998), Sadeghi et al. (2013) and Wang et al. (2007). Note that the definition of the knee joint angle in Gross et al. (1998) and in Wang et al. (2007) is in the reverse direction as the angle direction chosen in this work and in Sadeghi et al. (2013). In Wang et al. (2007) the ankle is not measured. In Fig. 5, the results from the presented model are compared to the results from literature with the correction of the angle direction.

In general, the sign and order of magnitude of the torques are comparable and close to what can be expected. However, patient-specificity can lead to differences between measurement sets, which can be seen in Fig. 5.

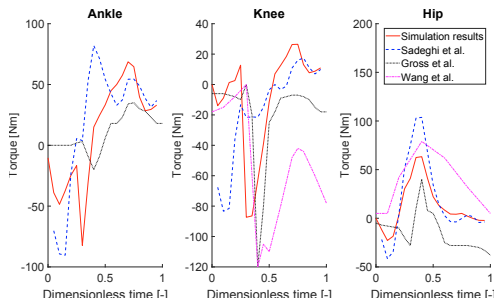


Fig. 5. Kinematic model validation.

3.2 The elderly

Fig. 6 shows the obtained torques for the STS movement of the complete model, i.e. the joint kinematics and the human policy. Using the simulator, it can be verified that a person of age is not able to perform the STS movement. In Fig. 7a, the relative error between the desired joint angles and the actual joint angles for a STS movement in the elderly is plotted. Note here that the error for the ankle joint does not reach zero, indicating that the patient has fallen.

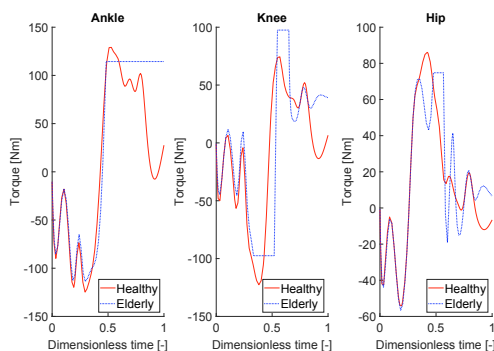
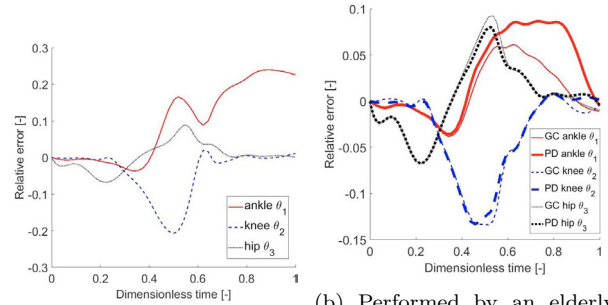


Fig. 6. Joint torques τ_1 , τ_2 and τ_3 for a healthy STS and a STS performed by an elderly.



(a) Performed by an elderly without orthosis. (b) Performed by an elderly with the orthosis (GC: gravity compensation, PD: control-based).

Fig. 7. Relative error of the joint angles during STS movement.

3.3 Closed-loop control

The relative error of the joint angles during the STS movement performed by an elderly wearing the orthosis with gravity compensation is shown in Fig. 7b, indicated with GC. The same is shown for the orthosis with a control-based strategy, indicated with PD. It becomes immediately clear that the final angles of the joint are equal to the reference. Thus both strategies are able to help an elderly with the STS movement.

The errors on the knee joint and the hip joint both reach an extremum but for a short instant. This maximal error is somewhat smaller for the control-based strategy than with the gravity compensation method. However, the maximal error on the ankle joint is larger for the control-based strategy compared to the gravity compensation method.

The torques observed at the human joints are plotted in Fig. 8. From Fig. 8 it can be concluded that the joint torque peaks with the orthosis have decreased, compared to the torques during the STS without an orthosis. This is valid for both methods for orthosis control. This shows that the muscles of the wearer are unburdened, which is an additional advantage for building up the physical training. Notice, that even with the orthosis saturation of the torques is reached, but that this does not impede the STS movement anymore.

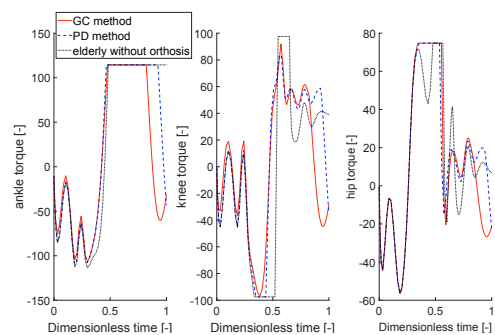


Fig. 8. Human torques for the different orthosis control methods (GC: gravity compensation, PD: control-based).

The results indicate that both methods can be simulated using the developed STS model and that future work can

be done to optimize the trajectory following with more advanced control strategies.

4. CONCLUSION

This work presents a full model of the joint kinematics of the lower limb combined with the human policy representing the brain and muscle interaction. This model is able to simulate both healthy as elderly patients. Its applicability is shown by implementing two popular control methods: i) gravity compensation and ii) a control-based method. The results show the validation of the model using measured joint torques found in literature. It can be concluded that the presented model can be used to test control architectures in a simulation environment such that the controller can be tested safely in an *in vivo* environment.

ACKNOWLEDGEMENTS

The authors acknowledge the contribution of H el ene Roelandt in this research.

REFERENCES

- Braun, D. and Goldfarb, M. (2009). A control approach for actuated dynamic walking in biped robots. *IEEE Transactions on Robotics*, 25(6), 1292–1303.
- Courrieu, P. (2008). Fast Computation of Moore-Penrose Inverse Matrices. *Neural Information Processing-Letters and Reviews*, 8. URL <http://arxiv.org/abs/0804.4809>.
- de Leva, P. (1996). Adjustments To Zatsiorsky-Seluyanov’s Segment Inertia Parameters. *Journal of Biomechanics*, 29(9), 1223–1230.
- DeVita, P. and Hortobagyi, T. (2000). Age causes a redistribution of joint torques and powers during gait. *Journal of Applied Physiology*, 88(5), 1804–1811. doi:10.1152/jap.2000.88.5.1804.
- dos Santos, A., Pavao, S., and Rocha, N. (2011). Sit-to-stand movement in children with cerebral palsy: A critical review. *Res Dev Disabil*, 32, 2243–2252.
- Esquenazi, A. and Talaty, M. (2019). *Atlas of Orthoses and Assistive Devices*, chapter Future Trends and Research in Orthoses, 448–450. Fifth Edit Elsevier Inc.
- Gorgey, A.S., Sumrell, R., and Goetz, L.L. (2019). Exoskeletal Assisted Rehabilitation After Spinal Cord Injury. In J.B. Webster and D.P. Murphy (eds.), *Atlas of Orthoses and Assistive Devices*, 440–447.e2. Elsevier Inc., fifth edit edition. doi:10.1016/b978-0-323-48323-0.00044-5. URL <https://doi.org/10.1016/B978-0-323-48323-0.00044-5>.
- Gross, M.M., Stevenson, P.J., Charette, S.L., Pyka, G., and Marcus, R. (1998). Effect of muscle strength and movement speed on the biomechanics of rising from a chair in healthy elderly and young women. *Gait and Posture*, 8(3), 175–185. doi:10.1016/S0966-6362(98)00033-2.
- Ljung, L. (1983). *System Identification: Theory for the User*. Prentice-Hall, Englewood Cliffs, NJ.
- Lv, G. and Gregg, R.D. (2018). Underactuated Potential Energy Shaping With Contact Constraints: Application to a Powered Knee-Ankle Orthosis. *IEEE Transactions on Control Systems Technology*, 26(1), 181–193. doi:10.1109/TCST.2016.2646319.
- Oddsson, L.I., Boissy, P., and Melzer, I. (2007). How to improve gait and balance function in elderly individuals—compliance with principles of training. *European Review of Aging and Physical Activity*, 4(1), 15–23. doi:10.1007/s11556-007-0019-9.
- Pirker, W. and Katzenschlager, R. (2017). Gait disorders in adults and the elderly: A clinical guide. *Wiener Klinische Wochenschrift*, 129(3–4), 81–95. doi:10.1007/s00508-016-1096-4.
- Rajasekaran, V., Vinagre, M., and Aranda, J. (2017). Event-based control for sit-to-stand transition using a wearable exoskeleton. In *International Conference on Rehabilitation Robotics (ICORR)*, 400–405. IEEE. doi:10.1109/ICORR.2017.8009280.
- Roebroeck, M., Doorenbosch, C., Harkaar, J., Jacobs, R., and Lankhorst, G. (1994). Biomechanics and muscular activity during sit-to-stand transfer. *Clin Biomech*, 9(4), 235–244.
- Sadeghi, M., Andani, M.E., Bahrami, F., and Parnianpour, M. (2013). Trajectory of human movement during sit to stand: A new modeling approach based on movement decomposition and multi-phase cost function. *Experimental Brain Research*, 229(2), 221–234.
- Schoene, D., Heller, C., Aung, Y., Sieber, C., Kemmler, W., and Freiberger, E. (2019). A systematic review on the influence of fear of falling on quality of life in older people: is there a role for falls? *Clin Interv Aging*, 14, 701–719. doi:10.2147/CIA.S197857.
- Sheng, Z., Iyer, A., Sun, Z., Kim, K., and Sharma, N. (2022). A hybrid knee exoskeleton using real-time ultrasound-based muscle fatigue assessment. *IEEE/ASME Transactions on Mechatronics*, 27(4), 1854–1862.
- Shepherd, M.K. and Rouse, E.J. (2017). Design and validation of a torque-controllable knee exoskeleton for sit-to-stand assistance. *IEEE/ASME Transactions on Mechatronics*, 22(4), 1695–1704.
- Wang, F.c., Yu, C.h., Lin, Y.l., and Tsai, C.e. (2007). Optimization of the Sit-to-Stand Motion. In *IEEE/ICME International Conference on Complex Medical Engineering*, 1248–1253.